Department of Electrical Engineering

National Taiwan University of Science and Technology

2021 First Semester Project

PROJECT REPORT

MIMO Antennas for Sub-6 GHz Mobile Phone Applications

Group：F01-1101

Members： 羅琦翔 Chi-Hsiang, Lo   Student Number：B10732017

李裕萌 Jason Li   Student Number：B10732038

Supervisor：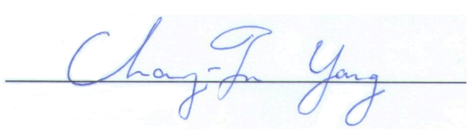 (Signature)

December 2021

Table of Contents

1. Introduction

1.1. General Background

The fifth-generation mobile communication system (5G) has many advantages such as higher transmission rate and shorter latency compared to the current 4G system. 5G works in either the sub-6 GHz bands or millimeter-wave. However, due to the limited space in mobile phones, it poses a challenge in simultaneously achieving high isolation and efficiency for the MIMO antenna system.

1.2. Purpose of Research

With the technology of 5G phone-making maturing, the space in mobile phones left for placing antennas became smaller. We chose our project on sub-6 GHz and used 3.5 GHz for resonance frequency. We aim to reduce the original antenna's height by nearly 30% (7mm to 5.4mm) while still maintaining S_{11} (Return Loss) under -10dB, S_{21} (Isolation) under -16dB and high efficiency.

1.3. Literature Review

In [1], a 2-antenna MIMO system based on compact self-decoupled antenna pairs is proposed. By placing two adjacent antenna elements of the antenna pair very close to each other and by arranging the two antenna elements to share one common coupled grounding branch, very good isolation can be obtained, as shown in Fig.1. The performance of the proposed self-decoupled MIMO system is confirmed by both simulation and measurement, as shown in Fig.2.

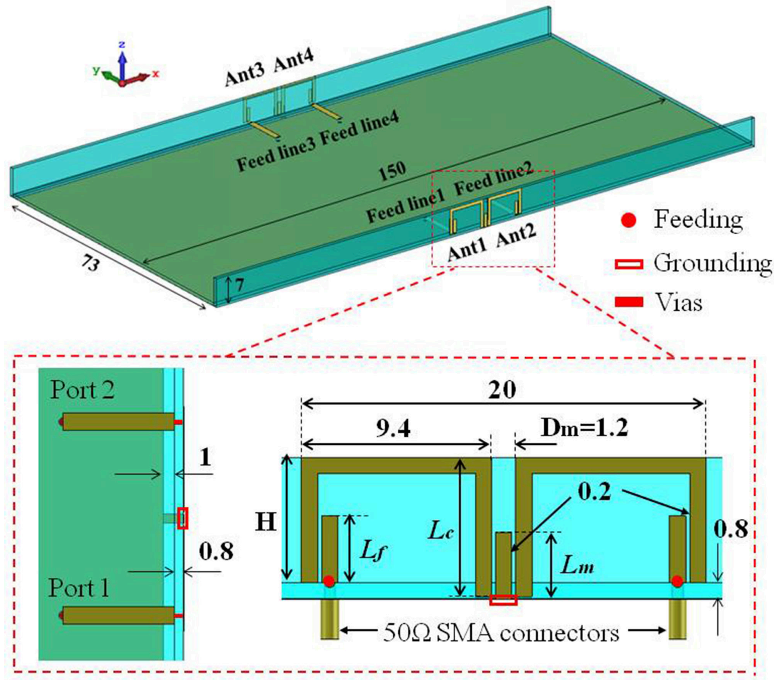

Fig. 1. Geometry of the 2-antenna MIMO system composed of two compact self-decoupled antenna pairs. All units are in millimeters [2].

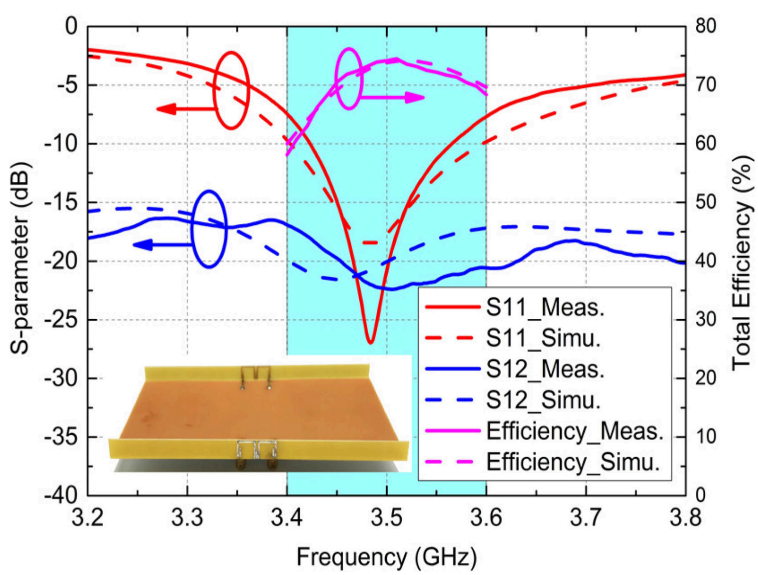

Fig. 2. Performance comparison between the simulated and measured results in terms of S-parameter and antenna total efficiency with H = 6.2 mm [2].

In [1], each antenna pair consists of two identical antenna elements, and each antenna element has an I-shaped feeding branch and a U-shaped radiating branch. The two identical antenna elements share a common grounding branch that is coupled with the U-shaped radiating elements.

To better understand the working principle of the proposed 2-antenna MIMO system, some parameter studies are given next.

When the value of the feeding rod, Lf, varies, the impedance matching and resonance frequency of the MIMO system change significantly, but the antenna isolation does not alter much, as shown in Fig. 3.

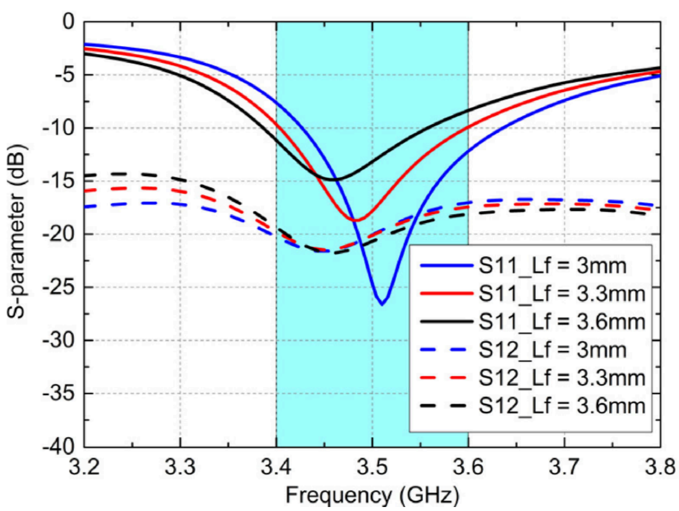

Fig. 3. Simulated S-parameter of the MIMO antenna varies as a function of Lm [2].

In Fig. 4, it shows that optimizing the height of the common grounding branch, Lm, can not only improve the isolation of the MIMO antenna pair, but it can also increase the effective length of the antenna element.

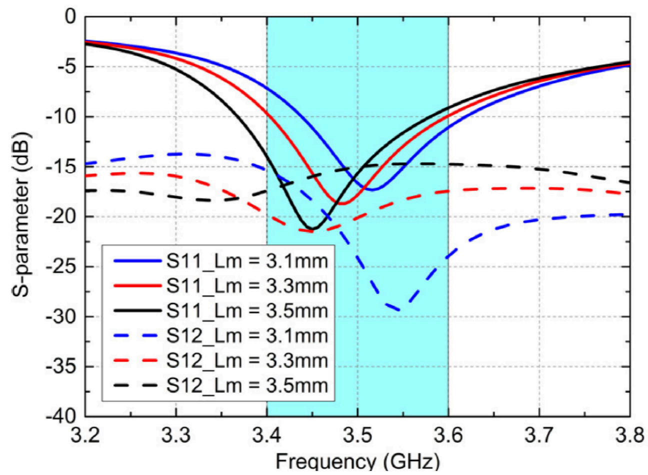

Fig. 4. Simulated S-parameter of the MIMO antenna varies as a function of Lm [2].

Fig. 5 shows insignificant current flows or couples from Ant1 to Ant2 when Lm = 3.0 mm. The antenna pair works as the proposed self-decoupled MIMO antenna pair when Lm ≥ 3.0 mm.

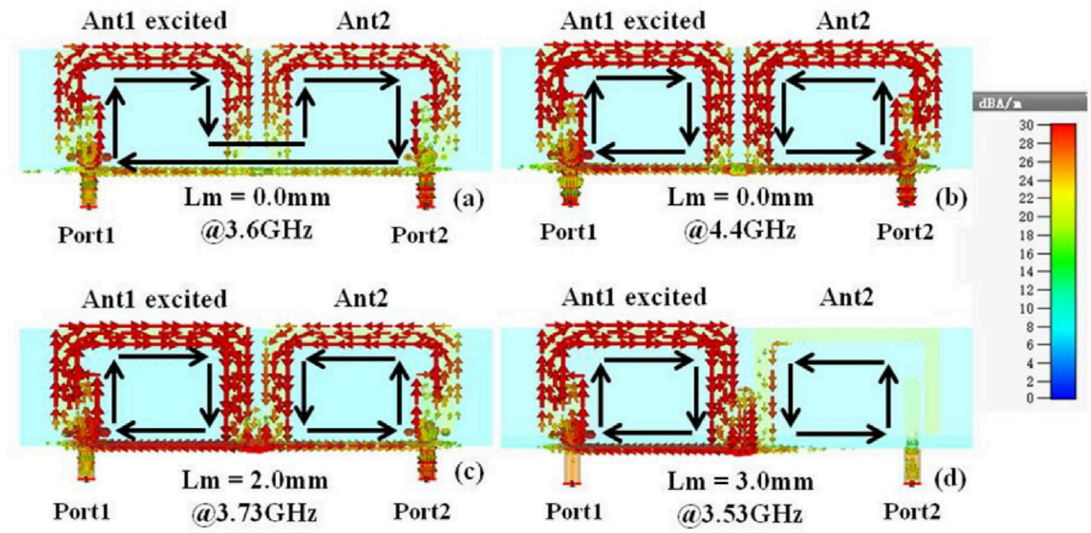

Fig. 5. Comparison of the simulated current distributions for different cases. (a) 3.6 GHz with Lm = 0.0 mm. (b) 4.4 GHz with Lm = 0.0 mm. (c) 3.73 GHz with Lm = 2.0 mm. (d) 3.53 Ghz with Lm = 3.0 mm [2].

2. The Compact 2-antenna MIMO System

We reduced the height by nearly 30% while using HFSS to simulate several different approaches and designs to enhance isolation, efficiency and bandwidth.

Original Antenna's height reduced from 7mm to 5mm:

To determine whether the original antenna [1] can achieve ideal S11 and S21 when the height is reduced by approximately 30%, we performed modified simulations, as shown in Fig. 6 & Fig. 7 based on the original model. The resonance frequency is around 3.9 GHz with the bandwidth of 600 MHz smaller than -6 dB, as shown in Fig. 8 & Fig. 9.

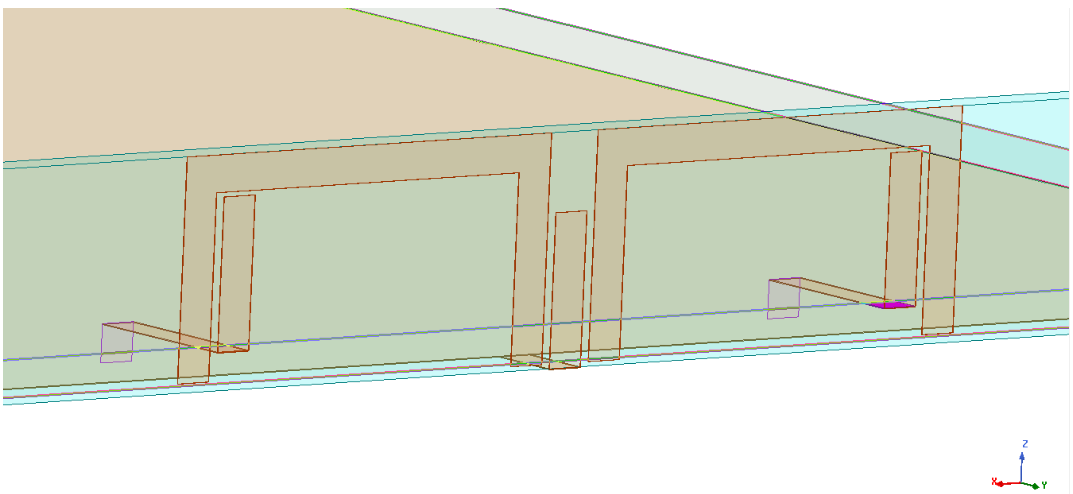

Fig. 6. Three-Dimensional view of the MIMO antenna pair

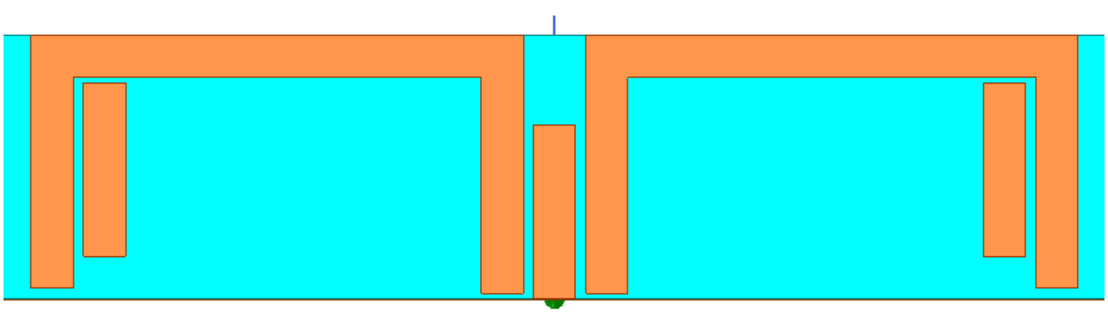

Fig. 7. Front view of the MIMO antenna pair

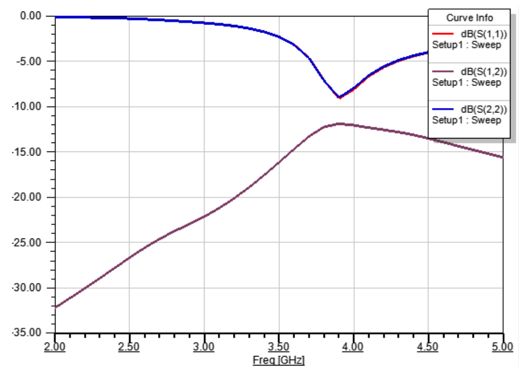

Fig. 8. S parameters of the MIMO antenna pair

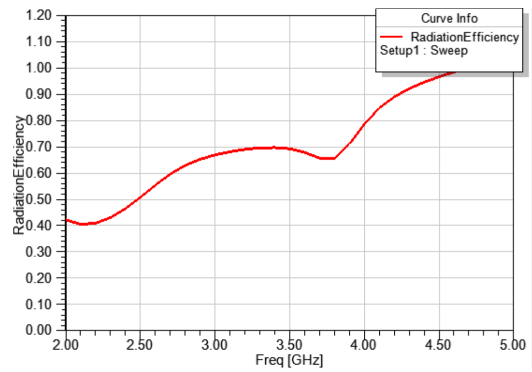

Fig. 9. Efficiency of the MIMO antenna pair

The original antenna possesses a circular polarization, as shown in Fig. 10. Therefore, in order to enhance the isolation between the two ports, we adopted several decoupling methods.

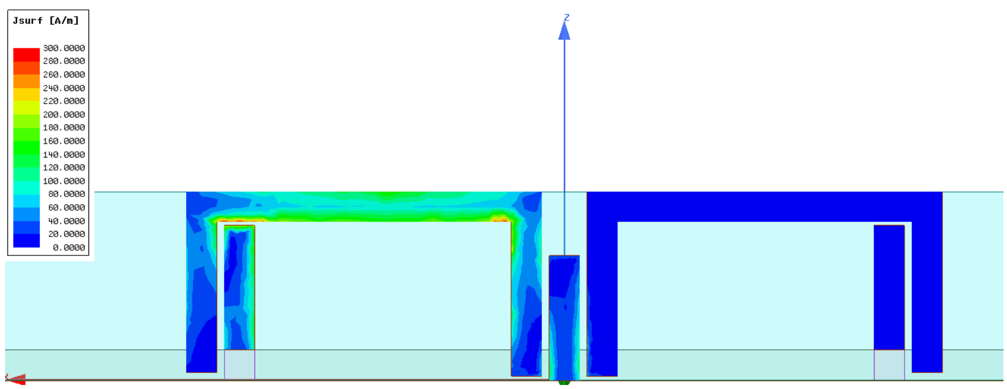

Fig. 10. Current Distribution of the original antenna

One method of decoupling is to use different designs and polarizations on the adjacent antenna. In that way, we expected to fully take out the middle isolation rod and still maintain a decent isolation. We implemented three different polarization designs for each antenna element and compared the results, these three designs are as follows: an Inverted F Antenna, an U-shaped combined with L-shaped Antenna, and the original U-shaped Antenna. However, in this report we are focusing on our design improvement.

3. Project Contributions

U-shaped antenna combined with L-shaped antenna:

Referencing the design in [1] and [2], we learned that the length of our antenna will impact the resonance frequency. Furthermore, we found several different approaches to expand the electrical length, such as altering the height of the middle isolation rod and adding the T-shape branch in [3]. Considering the manufacturing difficulty while still implementing the isolation rod in the design, we implemented a new way to place our ground plane, which is to place two ground planes on both the top and bottom with two isolation rods attached to it on both sides. The advantage is that it's much easier to manufacture, but the downside is the two copper planes will form a waveguide-like structure and may influence the antenna system parameters.

Our design is composed of a U-shaped element with a L-shaped monopole antenna printed separately on the different sides of the 0.8mm thick FR4 substrate, as shown in Fig. 11 & Fig. 12. The dimensions of the antenna system is 28.6mm × 5.4mm. Results in Fig. 13 verify that isolation lower than -16 dB can be achieved within the 3.4~3.6 GHz bandwidth. In addition, the radiation efficiency of 60% and current distribution were also simulated in Fig. 14 and Fig. 15.

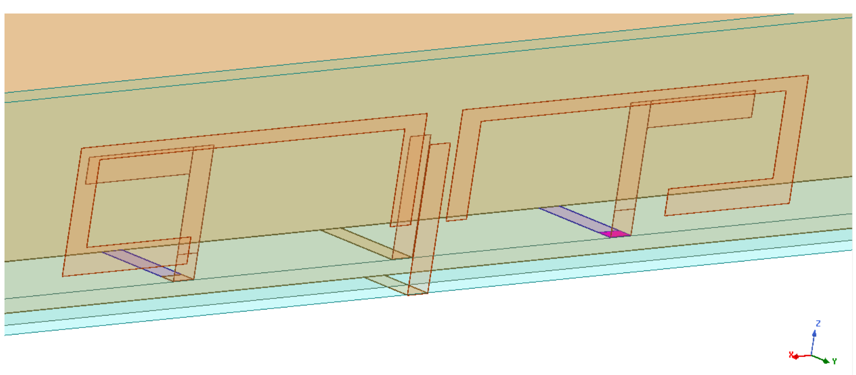

Fig. 11. Three-Dimensional view of the MIMO antenna pair

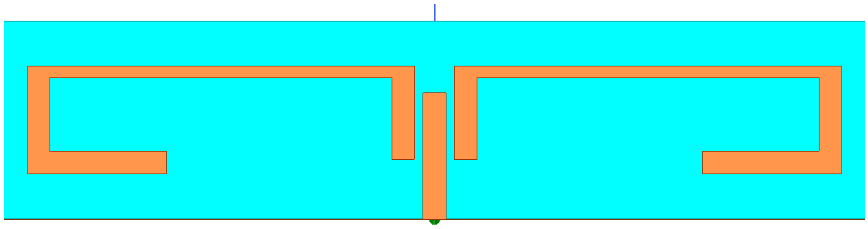

Fig. 12. Front view of the MIMO antenna pair

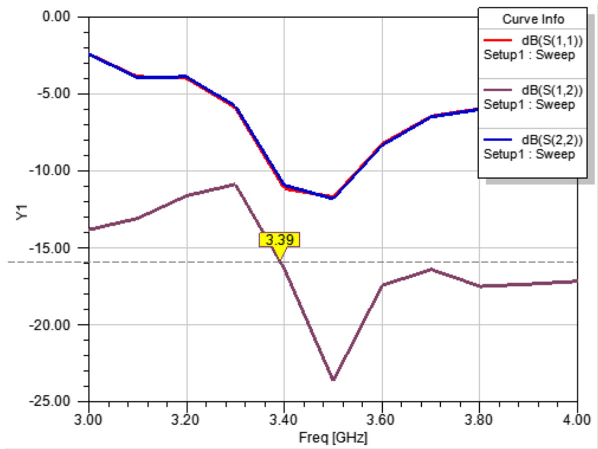

Fig. 13. S parameters of the MIMO antenna pair

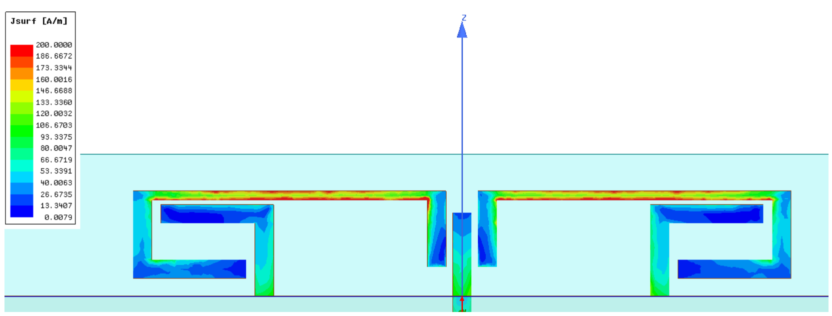

Fig. 14. Current distribution of the MIMO antenna pair

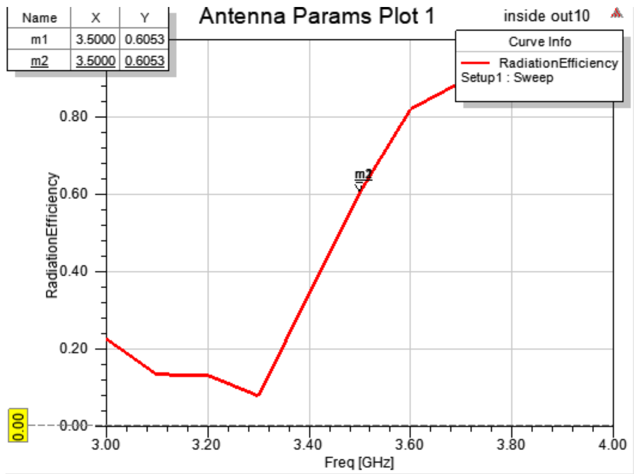

Fig. 15. Radiation efficiency of the MIMO antenna pair

4. Experimental Data

In order to connect the feedline with the cable easily, we dug out two slots on the sides of our system's ground plane while still keeping S_{11} stable, as shown in Fig.16 and Fig.17.

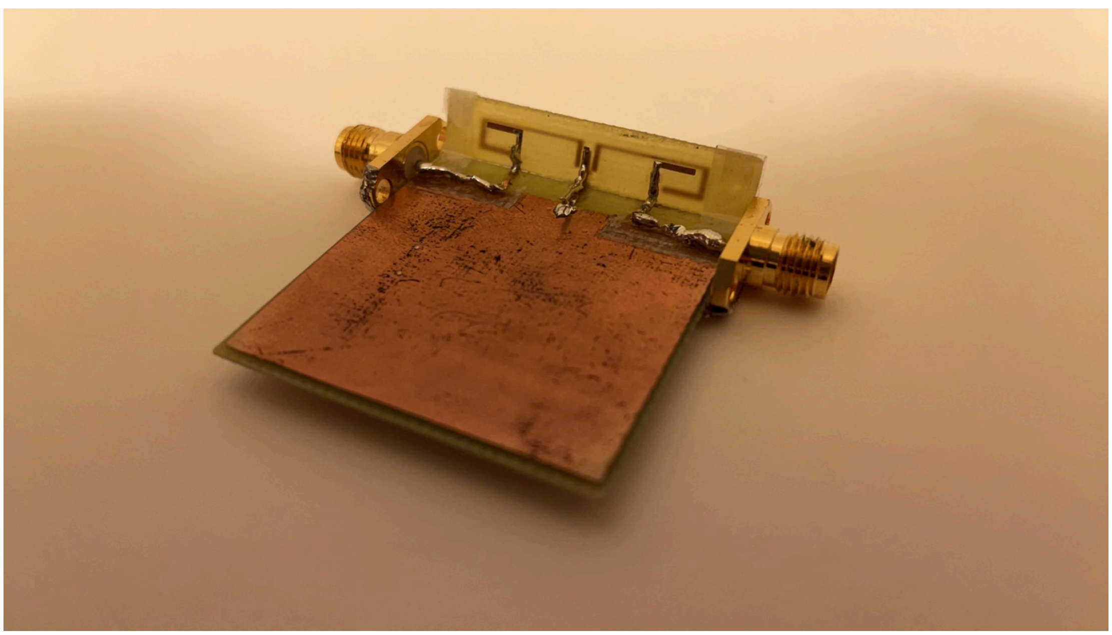

Fig. 16. Back view of the experiment antenna

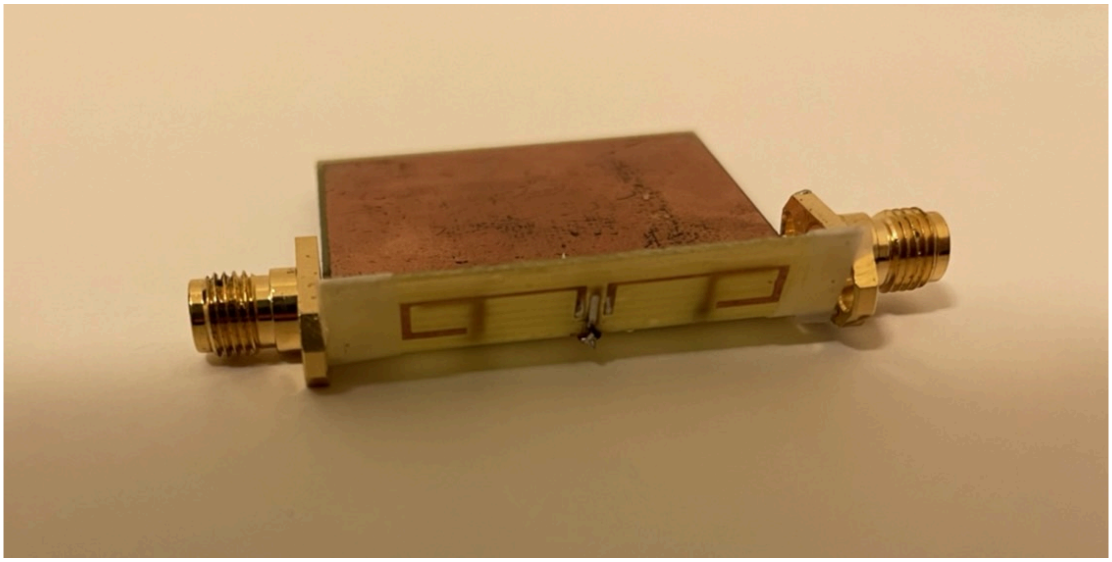

Fig. 17. Front view of the experiment antenna

Theoretically, the length of our feed line determines the input impedance of the system, as shown in the formula down below.

$$Z_{IN} = Z_0 \left[\frac{Z_L + j\, Z_0 \tan(\beta \ell)}{Z_0 + j\, Z_L \tan(\beta \ell)} \right]$$

- *Z_L is the termination impedance*
- *ℓ is line length.*
- *$\beta = 2\pi f / (V_P)$*

As we dug out a slot, it means that the length of our system's feed line is lengthened. Calculated by the formula above, the length of ℓ will not only affect S_{11}, but it will also affect S_{21} and even the efficiency as well. Therefore, it is our prime task to assure the input impedance from experiment will not deviate from our simulation.

For the S parameters measurements, we used the Keysight PNA-L Network Analyzer N52328, as shown in Fig.18.

Fig.18. Keysight PNA-L Network Analyzer N52328 used for S parameter measurements

Fig. 19. shows that port 1 has a resonance frequency of 3.75 GHz. The resonance frequency was off by 0.25 GHz, which may be the result of manufacturing and measurement errors. Manufacturing errors may include flawed soldering and front-back misalignment. Measurement errors may include calibration inaccuracy and environmental disturbance. Despite the offset of resonant frequency, results from the measurement were satisfying. From 3.38 GHz to 4 GHz, we passed the -10dB threshold which gives us a bandwidth of 0.62 GHz.

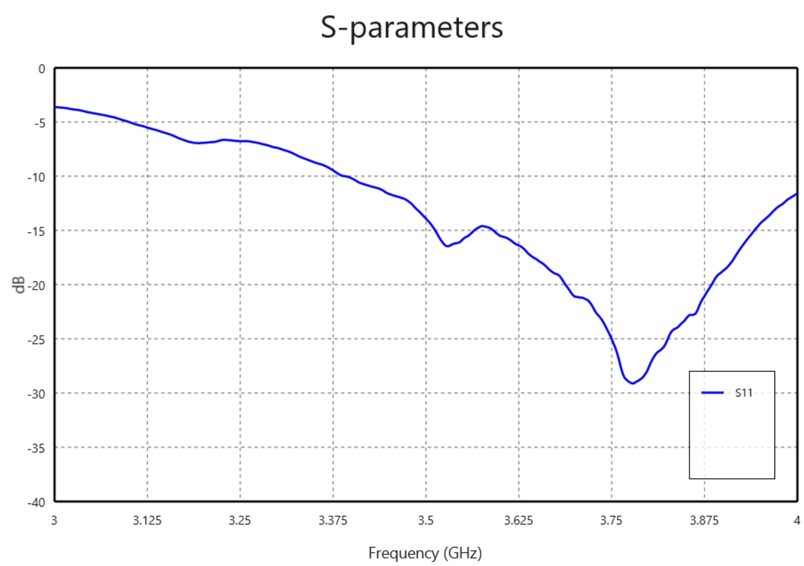

Fig. 19. S_{11} of the experiment antenna

In Fig. 20. it shows that port 2 possesses a resonance frequency of 3.6 GHz and a bandwidth of approximately 0.5 GHz while using the same -10dB as standard.

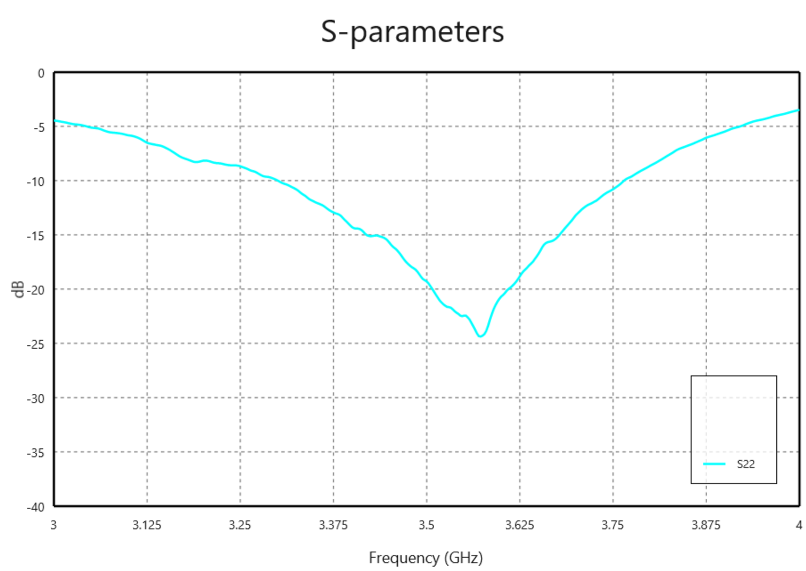

Fig. 20. S_{22} of the experiment antenna

With isolation less than -16 dB as our standard, Fig. 21. indicates our prototype antenna passes the standard for isolation.

Unfortunately, the efficiency from the experiment was 30%, which is half compared to our simulation. This might be the consequence of the soldering defects, inconsistent width of the feed line, and misalignment of the system substrate.

Fig. 21. S_{21} of the experiment antenna

To measure our antenna's near field distribution, we used the Spherical Near-Field Antenna Measurement Anechoic Chamber from NTUST, as shown in Fig.22. We ran a sweep from 3.0 GHz to 4.0 GHz with a step size of 0.1 GHz. The results of the measured radiation patterns are shown in Fig. 23~25..

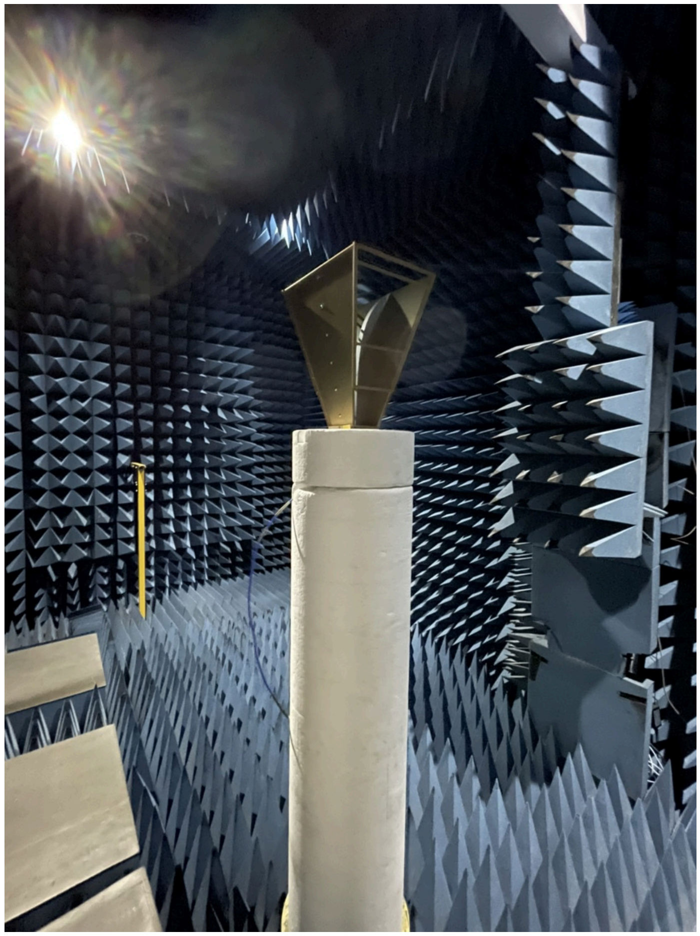

Fig. 22. Calibration process of the Spherical Near-Field Antenna Measurement Anechoic Chamber

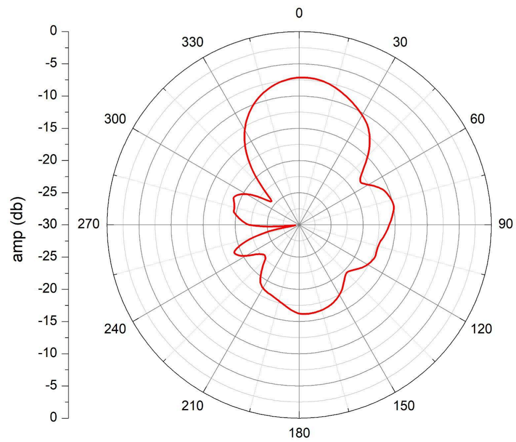

Fig. 23. Measured radiation pattern on the xoy plane

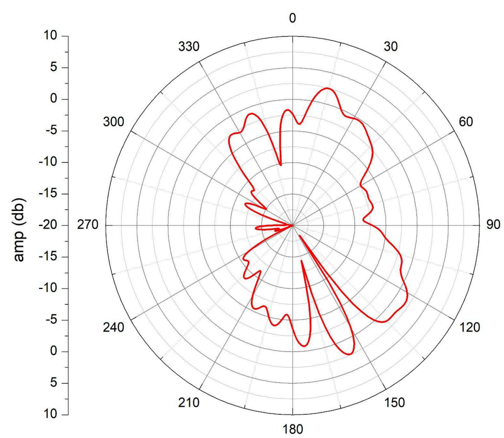

Fig. 24. Measured radiation pattern on the xoz plane

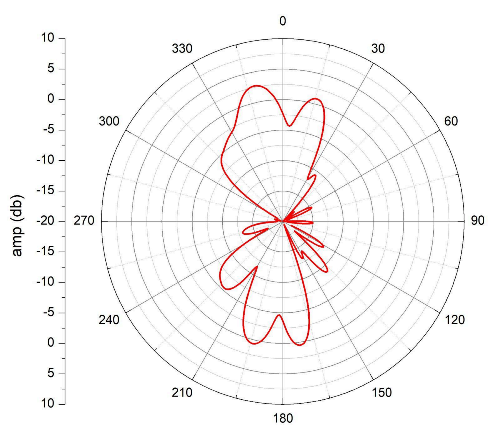

Fig. 25. Measured radiation pattern on the yoz plane

5. Conclusion

A 2-antenna MIMO system with the compact self-decoupled antenna pairs for 5G applications in mobile terminals is proposed. By sharing two common grounding branches for the two adjacent antennas of the antenna pair, quite good isolation can be obtained even when the two antennas are located very close to each other. Furthermore, the height of the original antenna was miniaturized from 7mm to 5.4mm. Because of the compact structure of our proposed antenna, along with high isolation and good antenna efficiency, it would be very useful for 5G MIMO applications in mobile terminals.

6. Future Development

In this project we tried out several methodologies to optimize the S-parameters while reducing the 2-antenna system's height. However, due to the limited knowledge we have, the width of the antenna was broadened. In the near future, we aim to reduce the width while maintaining the same isolation and efficiency.

7. Gantt Chart

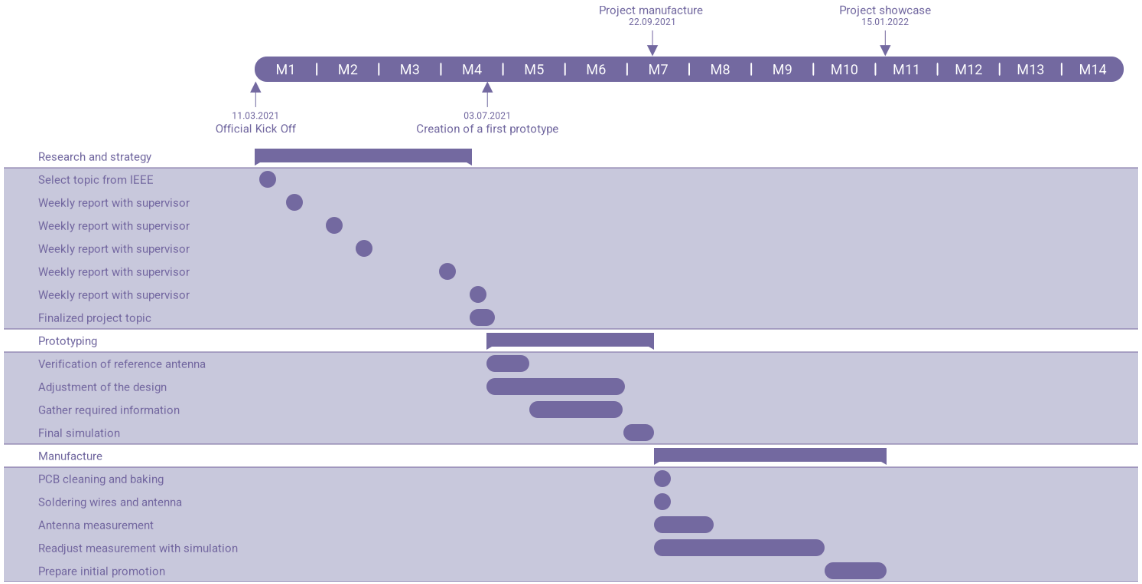

8. References

[1] Zhouyou Ren, Anping Zhao and Shengjie Wu "MIMO Antenna With Compact Decoupled Antenna Pairs for 5G Mobile Terminals," *IEEE Antennas and Wireless Propagation Letters*, vol. 18, no. 7, July 2019

[2] Hatte J.S. and Rupali B. Patil "Design Methods of MIMO Antenna for 5G New Radio Applications in Mobile Terminals-A Review," *International Journal on Emerging Technologies 11*: 738-745(2020)

[3] Anping Zhao , Senior Member, IEEE, and Zhouyou Ren "Size Reduction of Self-Isolated MIMO Antenna System for 5G Mobile Phone Applications," *IEEE Antennas And Wireless Propagation Letters*, vol. 18, no. 1, January 2019

9. Work Distribution

Antenna Design:	Jason Li、Chi-Hsiang, Lo
Antenna Simulation:	Jason Li、Chi-Hsiang, Lo
Simulation Analysis:	Jason Li、Chi-Hsiang, Lo
PCB cleaning and baking:	Jason Li、Chi-Hsiang, Lo
Antenna soldering:	Jason Li、Chi-Hsiang, Lo
Antenna measurement & adjustment:	Jason Li、Chi-Hsiang, Lo

10. Expense Table

FR4 board:	\$50 NTD
Copper sheet:	\$104 NTD
SMA jack:	\$320 NTD
HFSS software:	\$0 (Campus Software)
Total:	\$474 NTD